J. Condensed Matter Nucl. Sci. 13 (2014) 264–276

Research Article

Conventional Nuclear Theory of Low-energy Nuclear Reactions in Metals: Alternative Approach to Clean Fusion Energy Generation

Yeong E. Kim *

Department of Physics, Purdue University, West Lafayette, IN 47907, USA

Abstract

Low-energy nuclear reactions (LENRs) in metals are described using conventional nuclear theory based on the optical theorem formulation. It can be applied to both deuteron and proton induced LENRs. Cryogenic ignition of deuteron fusion in metal particles is proposed as an alternative approach to clean fusion energy generation.
 ISSN 2227-3123

Keywords: Deuteron fusion in metals, Nuclear theory, Nuclear transmutations, Optical theorem formulation

1. Introduction

Over the last two decades, there have been many publications reporting experimental observations of excess heat generation and anomalous nuclear reactions occurring in metals at ultra-low energies, now known as 'low-energy nuclear reactions'(LENRs). After a review of key experimental observations, theoretical explanations of the LENR phenomena will be described by conventional nuclear theory based on the optical theorem formulation of LENRs (OTF-LENRs) [1] and theory of Bose–Einstein condensation nuclear fusion (BECNF) in micro/nano-scale metal particles [2–11]. Proposed experimental tests of the basic assumption and theoretical predictions as well as potential application to cryogenic ignition of deuteron fusion in micro/nano-scale metal particles will be described [11,12].

The OTF-LENRs [1,2] can be applied to both conventional nuclear beam experiments and also to LENRs in metals. The BECNF theory [2–12] is merely one of many potential applications of the OTF-LENRs, which we will be exploring in future. The OTF-LENRs can also be applied to proton–nucleus transmutation reactions, etc. It can be applied possibly to biological transmutations

*E-mail: yekim@purdue.edu

 ISSN 2227-3123

2. Anomalous Experimental Results

2.1. D + D reaction channels in free space

The conventional deuterium fusion in free space proceeds via the following nuclear reactions:

$\{1\}$ D + D → p (3.02 MeV) + T (1.01 MeV),

$\{2\}$ D + D → n (2.45 MeV) + ^{3}He (0.82 MeV),

$\{3\}$ D + D → ^{4}He + γ (23.8 MeV).

The cross-sections for reactions $\{1\}$–$\{3\}$ are expected to be extremely small at low energies ($\leq$10 eV) due to the Gamow factor arising from Coulomb barrier between two deuterons. The measured cross-sections have branching ratios: $(\sigma\{1\}, \sigma\{2\}, \sigma\{3\}) \approx (0.5, 0.5, \sim 10^{-6})$.

Experimental values of the conventional hot-fusion cross section $\sigma(E)$ for reaction $\{1\}$ or $\{2\}$ have been conventionally parameterized as [13]:

$$\sigma(E) = \frac{S}{E} e^{-2\pi\eta} = \frac{S}{E} e^{-\sqrt{E_G/E}} \tag{1}$$

with

$$\eta = \frac{1}{2kr_B}, \quad r_B = \frac{\hbar^2}{2\mu e^2}, \quad \mu = m/2,$$

where $e^{-2\pi\eta}$ is known as the "Gamow factor", and E_G is the "Gamow energy" given by

$$E_G = (2\pi\alpha Z_d Z_d)\mu c^2/2 \quad \text{or} \quad \sqrt{E_G} \approx 31.39\sqrt{\text{keV}}$$

for the reduced mass $\mu = m/2$ for reactions $\{1\}$ or $\{2\}$.

The value E is measured in keV in the center-of-mass (CM) reference frame. The S-factor, $S(E)$, is extracted from experimentally measured values [14] of the cross section $\sigma(E)$ for $E \geq 4$ keV and is nearly constant [15]; $S(E) \approx$ 52.9 keV-barn, for reactions $\{1\}$ or $\{2\}$, in the energy range of interest here, $E \leq 100$ keV. The S-factor is known as "astrophysical S-factor" [13].

2.2. D + D Reaction channels in metals

From many experimental measurements by Fleischmann and Pons [16] in 1989, and many others [17–19] over 23 years since then, the following experimental observations have emerged from experimental results reported from electrolysis and gas-loading experiments. They are summarized below (as of 2011, not complete: exit reaction channels $\{4\}$–$\{6\}$ are defined below and are shown in Fig. 1):

(1) The Coulomb barrier between two deuterons are suppressed.
(2) Production of nuclear ashes with anomalous rates: $R\{4\} \ll R\{6\}$ and $R\{5\} \ll R\{6\}$.
(3) ^{4}He production commensurate with excess heat production, no 23.8 MeV γ-ray.
(4) Excess heat production (the amount of excess heat indicates its nuclear origin).
(5) More tritium is produced than neutron $R\{4\} > R\{5\}$.
(6) Production of hot spots and micro-scale craters on metal surface.
(7) Detection of radiations.

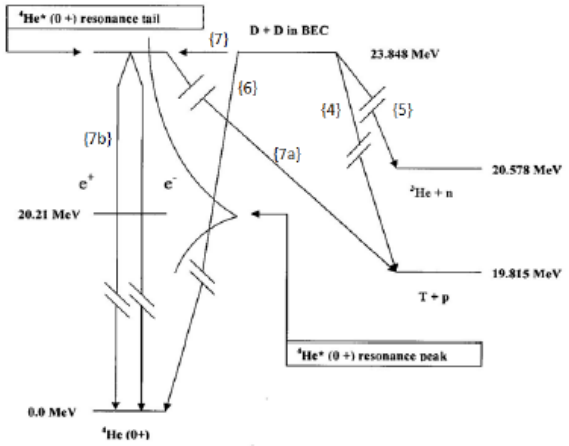

Figure 1. Exit reaction channels for D + D reactions in metal. Parallel bars indicate break in energy scale.

(8) "Heat-after-death".
(9) Requirement of deuteron mobility (D/Pd $>\sim 0.9$, electric current, pressure gradient, etc.).
(10) Requirement of deuterium purity (H/D $\ll 1$).

All of the above experimental observations are explained either quantitatively or qualitatively in terms of theory of BECNF in previous publications [2–12].

As shown in Fig. 1, at ambient temperatures or low energies ($\leq$10 eV), deuterium fusion in metal proceeds via the following reactions:

$\{4\}$ D(m) + D(m) $\rightarrow$ p(m) + T(m) + 4.03 MeV (m),

$\{5\}$ D(m) + D(m) $\rightarrow$ n(m)+^{3}He(m) + 3.27 MeV (m),

$\{6\}$ D(m) + D(m) $\rightarrow$ ^{4}He(m) + 23.8 MeV (m),

where m represents a host metal lattice or metal particle. Reaction rate R for $\{6\}$ is dominant over reaction rates for $\{4\}$ and $\{5\}$, i.e., R$\{6\} \gg$ R$\{4\}$ and R$\{6\} \gg$ R$\{5\}$.

3. Optical Theorem Formulation

In this section, we introduce a low-energy "partial-wave" optical theorem and use it to develop the optical theorem formulation (OTF) of LNERs.

3.1. Optical theorem for positive energy scattering

The conventional optical theorem first introduced by Feenberg [20] is given by

$$\sigma_{\mathrm{t}} = \frac{4\pi}{k} \mathrm{Im} f(0), \tag{2}$$

which shows that the total cross section is related to the elastic scattering amplitude in the forward direction, $f(0)$. To avoid complications associated with the singularity of the forward Coulomb scattering amplitude $f_{\rm c}$ (0) as in the case of the conventional optical theorem, for two-potential scattering involving two charged nuclei, we used a different formulation based on a partial-wave optical theorem involving angle-integrated and/or angle-independent quantities to obtain the following optical theorem formula [1]

$$\text{Im } f_l^{n(\text{el})} \approx \frac{k}{4\pi}\sigma_l^{\rm r}, \tag{3}$$

where $f_l^{n(\text{el})}$ and $\sigma_l^{\rm r}$ are the l-th partial wave nuclear elastic scattering amplitude and reaction cross-section, respectively. The above formula is rigorous at low energies.

The elastic scattering amplitude can be written in terms of t-matrix as

$$f_l^{n(\text{el})} = -\frac{2\mu}{\hbar^2 k^2}\langle \psi_l^{\rm c} \,|t_l|\, \psi_l^{\rm c}\rangle, \tag{4}$$

where $\psi_l^{\rm c}$ is the Coulomb wave function for scattering between two charged particles. From Eqs. (3) and (4), we obtain the optical theorem formula for the dominant s-wave state as :

$$\frac{k}{4\pi}\sigma^{\rm r} = -\frac{2\mu}{\hbar^2 k^2}\langle \psi_0^{\rm c} \,|\text{Im}\, t_0|\, \psi_0^{\rm c}\rangle \tag{5}$$

and

$$\sigma^{\rm r} = \frac{S}{E}{\rm e}^{-2\pi\eta} \quad \text{with } \text{Im}\, t = -\tfrac{Sr_{\rm B}}{4\pi^2}\delta(\vec{r})\,. \tag{6}$$

The reaction rate is given by

$$R = v\sigma^{\rm r} = -\langle \psi^{\rm c} \,|\text{Im } V|\, \psi^{\rm c}\rangle \tag{7}$$

with Fermi potential

$$\text{Im}\, V = -\, A\delta(\vec{r}_{ij}), \quad A = \left(\frac{2}{\hbar}\right)\frac{Sr_{\rm B}}{\pi},$$

where S is related to the nuclear force strength and the delta-function represents the short-range nature of the nuclear force.

3.2. Generalization to LENRs in metals

The above result (7) can be generalized to D + D fusion reactions in metals to obtain

$$R_{\rm t} = -\frac{2}{\hbar}\frac{\Sigma_{i<j}\langle\psi \left|\text{Im } V_{ij}^{\rm F}\right| \psi\rangle}{\langle\psi|\psi\rangle} \tag{8}$$

with Fermi potential

$$\text{Im}\, V_{ij}^{\rm F} = -\frac{A\hbar}{2}\delta(\vec{r}_{ij}), \quad A = \left(\tfrac{2}{\hbar}\right)\tfrac{Sr_{\rm B}}{\pi}$$

Ψ is the bound-state solution of of the many-body Schroedinger equation

$$H\Psi = E\Psi \tag{9}$$

with

$$H = T + V^{\text{confine}} + V^{\text{Coulomb}} \quad . \tag{10}$$

The above general formulation can be applied to (i) D + D reactions in metals, (ii) proton–nucleus transmutations, etc. It could also possibly applied to (iii) biological transmutations. For each case of (i)–(iii), an appropriate Hamiltonian is to be chosen for Eqs. (9) and (10). To be realistic to a chosen physical system, H could include many degrees of freedom for electrons, metal lattice structures, etc. However, we may have to choose a simpler model Hamiltonian for which Eq. (9) can be solved approximately.

3.3. Importance and significance of OTF-LENRs

It is important to note differences between Eqs. (7) and (8). Equation (7) is for nuclear reactions at positive energies (such as for nuclear scattering experiments using beam of nuclei), while Eq. (8) is for nuclear reactions between two nuclei in a bound state (such as deuterons bound in a metal). In the past, Eq. (7) is inappropriately used to argue that LENRs in metals are impossible. It should be emphasize that the use of Eq. (8) is more appropriate for LENRs in metals.

4. Bose–Einstein Condensation Nuclear Fusion Theory

In this section, as an application of the OTF-LENRs (Eqs. (8)–(10)), we describe theory of BECNF.

4.1. Deuteron mobility in metals

Experimental proof of proton (deuteron) mobility in metals was first demonstrated by Coehn in his hydrogen electro-migration experiment [21,22]. A theoretical explanation of Coehn's results [21,22] is given by Isenberg [23]. The Coehn's results are not well known in review articles and textbooks. Velocity distributions of protons (dueterons) in metal have not been measured as a function of temperatures.

4.2. Theory

For applying the concept of the BEC mechanism to deuteron fusion in a micro/nano-scale metal particle, we consider N identical charged Bose nuclei (deuterons) confined in an ion trap (or a metal grain or particle). Some fraction of trapped deuterons are assumed to be mobile as discussed above. The trapping potential is 3-dimensional (nearly sphere) for micro/nano-scale metal particles, or quasi-two-dimensional (nearly hemi-sphere) for micro-scale metal grains, both having surrounding boundary barriers. The barrier heights or potential depths are expected to be an order of energy ($\leq$1 eV) required for removing a deuteron from a metal grain or particle. For simplicity, we assume an isotropic harmonic potential for the ion trap to obtain order of magnitude estimates of fusion reaction rates. N-body Schroedinger equation is given by Eq. (9) with the Hamiltonian H for the system given by

$$H = \frac{\hbar^2}{2m}\sum_{i=1}^{N}\Delta_i + \frac{1}{2}m\omega^2\sum_{i=1}^{N}r_i^2 + \sum_{i<j}\frac{e^2}{|\mathrm{r}_i - \mathrm{r}_j|} \quad (11)\,, \tag{11}$$

where m is the rest mass of the nucleus.

The approximate ground bound-state (GBS) solution of Eq. (9) with H given by Eq. (11) is obtained using the equivalent linear two-body method [4–6]. The use of an alternative method based on the mean-field theory for bosons yields the same result (see Appendix in [3]). Based on the optical theorem formulation of low energy nuclear reactions [1], the ground-state solution is used in Eq. (8) to derive the approximate theoretical formula for the deuteron–deuteron fusion rate in an ion trap (micro/nano-scale metal grain or particle). The detailed derivations are given elsewhere [2,3].

4.3. Reaction rate

Our final theoretical formula for the total fusion rate $R_{\rm t}$ for large N case is given by [2,3]

$$R_t = \frac{1}{4}\left(\frac{3}{\pi}\right)^{1/2} SB\Omega V n_{\rm D}^2, \tag{12}$$

where $B = 2\hbar/(\pi m e^2) = 1.4 \times 10^{-18}\text{cm}^3/(\text{sec-keV-barn})$, S is the S-factor for the nuclear fusion reaction between two deuterons, $n_{\rm D}$ is the deuteron number density, and V is the total volume. For D(d,p)T and D(d,n)^{3}He reactions, we have $S \approx 55$ keV-barn. We expect also $S \approx 55$ keV-barn or larger for reaction {6}. Only two unknown parameters are (i) the probability of the ground bound-state (GBS) occupation, Ω, and (ii) the S-factor. Equation (12) shows that the total fusion rates, $R_{\rm t}$, are maximized when $\Omega \approx 1$.

Equation (12) was derived analytically (no numerical calculations were involved). Equation (12) provides an important result that nuclear fusion rates $R_{\rm t}$ for large N case do not depend on the Gamow factor in contrast to the conventional theory for two-body nuclear fusion in free space. There is a simple classical analogy of the Coulomb field suppression. For an uniform spherical charge distribution, the Coulomb field diminishes toward the center and vanishes at the center.

4.4. Reaction mechanism

For a single trap (or metal particle) containing a large number N of deuterons, the deuteron–deuteron fusion can proceed with the two reaction channels {6} and {7}. We will discuss {6} in this section. {7} will be discussed in the next section.

For the large N case, the deuteron–deuteron reaction {6} in a GBS proceeds via

$$\{6\}\quad \Psi_{\rm GBS}\{(\text{D}+\text{D})+(N-2)\text{D}'\text{s}\} \rightarrow \quad \Psi^*_{\rm GBS}\{^4\text{He}+(N-2)\text{D's}\}(Q = 23.84\ \text{MeV}),$$

where the Q-value of 23.84 MeV is shared by ^{4}He and all D's in a GBS state, thus maintaining the momentum conservation in the final state. This implies that the deuteron GBS state undergoes a micro/nano-scale explosion ("micro-explosion" or "nano-explosion"). For a micro/nano-scale metal particle of 10 nm diameter containing $\sim 3.6 \times 10^4$ deuterons, each deuteron or ^{4}He will gain only ~ 0.7 keV kinetic energy, if the excess kinetic energy of 23.84 MeV is shared equally. For a larger metal particle, $\sim$0.7 keV is further reduced. This mechanism can provide an explanation for constraints imposed on the secondary reactions by energetic ^{4}He, as described by Hagelstein [24].

Furthermore, as these deuterons slow down in the host metal, they can release electrons from the host metal atoms, thus providing extra conduction electrons which may reduce the resistivity of the host metal.

Other exit channels, {4} and {5}, are expected to have much lower probabilities than that of the exit channel {6}, since both {4} and {5} involve centrifugal and Coulomb barrier transmissions of exit particles in the exit channels, while {6} does not, thus providing a theoretical explanation for the observation (2).

4.5. Role of Bose–Einstein condensation of deuterons

For BECNF processes, Bose–Einstein condensation of deuterons in metal is not required, but desirable for enhancing the fusion reaction rates as discussed below.

For $0.5 < \Omega < 1.0$, the GBS becomes a BEC state while for $\Omega < 0.1$ we have a GBS. For experimental results with very slow reaction rates observed so far, we have GBSs with $\Omega \ll 0.1$. For making Ω larger to improve reaction rates for scaling up the reaction rates and also improving reproducibility, it will require cooling (1) by lowering temperatures using coolants, or (2) by removing high velocity particles (evaporation cooling) with application of pressure gradients or with application of EM field gradients (including laser), etc.

5. Anomalous Tritium and Neutron Production

There have been many reports of anomalous tritium and neutron production in deuterated metal from electrolysis experiments [25–29] and gas/plasma loading experiments [30–36]. The reported branching ratio of $R(T)/R(n)$ ranges from 10^7 to 10^9 in contrast to the conventional free-space reactions branching ratio of $R\{1\}/R\{2\} \approx 1$. In this paper, we consider reaction rates for two exit channels to ^{4}He (0+, 0, 0.0 MeV) and ^{4}He*(0+, 0, 20.21 MeV) states.

5.1. Sub-threshold resonance reaction channel

In this section, we present a theoretical explanation of observed anomalous tritium production based on the BECNF theory, utilizing a sub-threshold resonance (STR) state ^{4}He* (0+) at 20.21 MeV with a resonance width of Γ(T + p) = 0.5 MeV [37] as shown in Fig. 1.

For the entrance channel {7}, exit channels are {7a} and {7b} as described below:

{7} Ψ_{GBS} { (D + D)+ (N - 2)Ds} $\rightarrow \Psi^*$ {^{4}He* (0+,0) + ($N-2$)Ds} ($Q = 0.0$ MeV),

{7a} ^{4}He*(0^+, STR, 23.85 MeV) $\rightarrow$ T(1.01 MeV) + p(3.02 MeV),

{7b} ^{4}He*(0^+, STR, 23.85 MeV) $\rightarrow$ ^{4}He(0^+, g.s., 0.0 MeV) + e^+ e^- pair.

5.2. Anomalous tritium production

For this section (Eqs. (13)–(15)), we use a new energy level scale which sets $E = 0$ for (D + D) state, and $E = -23.85$ MeV for the ^{4}He ground state. Q-value remains same since $Q = E_i - E_f$.

It is important to note that reaction {6} cannot occur in free space due to the momentum conservation, while reaction {7} can occur with $Q = 0$ in free space without violating the momentum conservation, due to the resonance width of Γ(T+p) = 0.5 MeV [37] for the 20.21 MeV state of ^{4}He*.

Reaction {7} can proceed via a sub-threshold resonance reaction [38,39]. The cross section for the sub-threshold resonance reaction is given by Breit–Wigner expression [39]

$$\sigma(E) = \pi \lambda\!\!\!^{-2} w \frac{\Gamma_1(E)\,\Gamma_2}{(E - E_R)^2 + (\Gamma/2)^2}, \tag{13}$$

where $\lambda\!\!\!^{-} = \lambda/2\pi$, $\lambda = h/mv$ (de Broglie wavelength), w is a statistical factor, E_R is the sub-threshold resonance energy. Γ_2 is a partial decay width and Γ is the total decay width to the final states. If E is measured from the threshold energy $E = 0$ of (D + D) state, E_R = (20.21 MeV–23.85 MeV) = – 3.64 MeV.

After combining Eq. (1) with Eq. (13), the $S(E)$ can be written

$$S(E) = E e^{\sqrt{E_G}/\sqrt{E}} \pi \lambda^2 w \frac{\Gamma_1(E)\,\Gamma_2}{(E - E_R)^2 + (\Gamma/2)^2} \tag{14}$$

from Eq. (14), we obtain the $S(E)$ factor near zero energy as [38]

$$\begin{aligned} S(E) &= \frac{\pi^2\hbar^4}{4\mu^2 R_n^2} \frac{1}{K_1^2(x)} w\theta_0^2 F_{BW}(E) \\ F_{BW}(E) &= \frac{\Gamma_2}{(E-E_R)^2+(\Gamma/2)^2} \end{aligned} \tag{15}$$

where μ is the reduced mass in units of atomic mass unit (931.494 MeV), R_n is the nuclear radius, and $K_1(x)$ is the modified Bessel function of order unity with argument

$$x = (8Z_1 Z_2 e^2 R_n \mu/\hbar^2)^{1/2}$$

.

We note that $F_{BW}(E_R)$ is a maximum at $E = E_R = -3.64$ MeV. At $E = 0$, $F_{BW}(0)$ is reduced to $F_{BW}(0) = 0.47 \times 10^{-2} F_{BW}(E_R)$. Equation (15) shows that the $S(E)$ factor has a finite value at $E = 0$ and drops off rapidly with increasing energy E. θ_i^2 is the reduced width of a nuclear state, representing the probability of finding the excited state in the configuration i, and the sum of θ_i^2 over i is normalized to 1. The dimensionless number θ_i^2 is generally determined experimentally and contains the nuclear structure information. $S(E)$ factors are calculated from Eq. (15) using $E = 0$ at a tail of the ^{4}He* (0^+,0) resonance at 20.21 MeV. $E = 0$ corresponds to 23.85 MeV above ^{4}He (0^+,0) ground state. The calculated $S(E)$ can be used in Eq. (12) to obtain the total fusion reaction rate. We will estimate $S(E)$ factors for the decay channels, {7a} and {7b}, using Eq. (15) in the following.

For the decay channel {7a}, $\Gamma_2 = \Gamma_a = 0.5$ MeV [37]. When this value of Γ_2 is combined with other appropriate inputs in Eq. (15), the extracted S-factor for the decay channel {7a} is S{7a} $\approx 1.4 \times 10^2 \theta_0^2$ keV-barn for $E \approx 0$. Since (^{3}He + n) state has a resonance width of Γ_2 (^{3}He + n) = 0 [37], this value of S{7a} may provide an explanation of the reported branching ratio of R(T)/R(n) $\approx 10^7 - 10^9$ [30–36] or R(n)/R(T) $\approx 10^{-7} - 10^{-9}$. If we assume S{6} ≈ 55 keV-b (this could be much larger), we expect the branching ratio R{7a}/R{6}= R(T)/R(^{4}He) $\approx 2.6\theta_0^2 \approx 2.6 \times 10^{-6}$ if $\theta_0^2 \approx 10^{-6}$. Experimental measurements of R(T)/R(^{4}He) are needed to determine θ_0^2. If S{6} (=S(^{4}He)) is determined to be larger from future experiments, R(T)/R(^{4}He) is reduced accordingly.From a previous estimate [9], we have theoretical prediction that R(n)/R(^{4}He) $< 10^{-11}$. Combining this with the above theoretical prediction of R(T)/R(^{4}He) $\approx 2.6\,\theta_0^2$, we have R(n)/R(T) $< 0.38 \times 10^{-11}/\theta_0^2$. If we assume $\theta_0^2 \approx 10^{-6}$, we have R(n)/R(T) $< 0.38 \times 10^{-5}$, which is consistent with reported values of $10^{-7} - 10^{-9}$.

5.3. Internal e^+e^- pair conversion

For the decay channel {7b} ($0^+ \rightarrow 0^+$ transition), γ-ray transition is forbidden. However, the transition can proceed via the internal e^+e^-pair conversion. The transition rate for the internal electron pair conversion is given by

$$\omega = \frac{1}{135\pi}\left(\frac{e^2}{\hbar c}\right)^2 \frac{\gamma^5}{\hbar^5 c^4} R_N^4, \qquad R_N^2 = \left|\left\langle \psi_{exc}, \sum_i r_i^2 \psi_{norm} \right\rangle\right| \tag{16}$$

where γ is the transition energy. Equation (16) was derived by Oppenheimer and Schwinger [40] in 1939 for their theoretical investigation of $0^+ \rightarrow 0^+$ transition in ^{16}O. The rate for the internal electron conversion is much smaller by many order of magnitude. For our case of $0^+ \rightarrow 0^+$ transition {7b}, we obtain $\omega \approx 1.75 \times 10^{13}$/s, and $\Gamma_b = \hbar\omega \approx 1.15 \times 10^{-2}$ eV using appropriate inputs in Eq. (16). Using $\Gamma_2 = \Gamma_b = 1.15 \times 10^{-2}$ eV in Eq. (15), the extracted S-factor for decay channel {7b} is $S\{7b\} \approx 3.3 \times 10^{-6}\theta_0^2$ keV-barn for $E \approx 0$, yielding a branching ratio, $R\{7b\}/R\{7a\} \approx S\{7b\}/S\{7a\} \approx 2.4 \times 10^{-8}$. Experiments are needed for testing this predicted branching ratio.

5.4. Anomalous neutron production

Experimental observation of $R(n)/R(T) \approx 10^{-7} - 10^{-9}$ [31–37] is anomalous since we expect $R(n)/R(T) \approx 1$ from "hot" fusion reactions, {1} and {2}. In this section, we explore nuclear reactions producing neutrons at anomalously low rates.

There are three possible processes that can produce neutrons:

The first process is the secondary "hot" fusion reaction {2} producing 2.45 MeV neutrons. The rate for this secondary reaction is extremely small, $R\{2\}/R\{6\} = R(n)/R(^4He) < 10^{-11}$, as shown previously [9].

The second process is a 3D BECNF reaction:

$$\{8\} \quad D + D + D \text{ (in BEC state)} \rightarrow n + p + {}^4He + 21.6 \text{ MeV}$$

This reaction is a secondary effect since the probability for {8} is expected to be much smaller than the 2D BECNF reaction {6}.

The third process is a "hot" fusion reaction

$$\{9\} \quad T + D \rightarrow n + {}^4He + 17.6 \text{ MeV}\,,$$

which is induced by 1.01 MeV T produced from reaction {7a}. Since the cross-section for reaction {9} is large and is a maximum (several barns) at $E_D \sim 100$ keV [41], neutrons from this process may contribute substantially to the branching ratio $R(n)/R(T) = 10^{-7} - 10^{-9}$.

Energetic neutrons from the third process {9} described above could induce the following reactions:

$$\{10\} \quad {}^{12}C\,(n, n')\,3^4He, \qquad {}^{12}C\,(n, n'\alpha)\,{}^8Be\ \left({}^8Be \rightarrow 2^4He\right), \text{ etc}\,.$$

as reported recently by Mosier-Boss et al. [42].

To test the above theoretical interpretation, based on the third process {9}, we need to measure/detect (i) tritium production, (ii) Bremsstrahlung radiations from energetic electrons going through metal, (iii) 0.51 MeV γ-rays from e^+e^- annihilation, (iv) energetic electrons from e^+e^- pair production, (v) γ-rays from the following reaction:

$$\{11\} \quad n + D \rightarrow T + \gamma + 6.257 \text{ MeV},$$

and (vi) γ-rays from reaction {12} induced by 0.3 MeV protons from {7a}:

$$\{12\} \quad p + D \rightarrow {}^3He + \gamma + 5.494 \text{ MeV}$$

The cross-section for {11} is ~0.5 mb with thermal neutrons.

6. Experimental Observation of Formation of Micro-craters

6.1. Experimental observations

There have been many reports of experimental observation of micro-craters [31,43,44]. In the following, estimates of energetics involved in a micro-crator formation observed by Szpak et al. [43] is presented.

6.2. Estimates of energetics

For the micro-crator shown in Fig. 2, we have the ejecta volume of $V = 1.6 \times 10^{-8}\text{cm}^3$ which contains 1.1×10^{15} deuterons, corresponding to $N_{\text{moles}} = 1.8 \times 10^{-9}$ moles of deuterons. The total energy E_{T} required for vaporization is $E_{\text{T}} = 6.5 \times 10^{-4}$ J. Since $Q = 23.8$ MeV per nuclear reaction, the total number N_{R} of D + D reactions is $N_{\text{R}} = E_T/Q = 1.7 \times 10^8$ DD reactions. Explosion time estimated from Eq. (12) is $\sim 1.2 \times 10^{-13}$ s/Ω.

7. Proposed Experimental Tests

BECNF theory is based on a physical observation of deuterons mobility in a metal grain/particle which may lead to possibility of forming a Bose–Einstein condensate of deuterons in metals. Two types of experimental tests (Proposed Experiments 1 and 2) are proposed as experimental tests of this possibility of observing BEC of deuterons in metals. For both types of experiments, the dependences on the temperature and pressure are to be measured. In addition, Proposed Experiment 3 is proposed to probe possibilities of cryogenic ignition of deuterons loaded in micro/nano-scale metal particles.

7.1. Proposed experiment 1

As is the case for the atomic BEC experiments, experiments are proposed to measure the velocity distribution of deuterons in metal. An enhancement of low-velocity deuterons in the deuteron velocity distribution is expected when the BEC of deuterons occurs. Inelastic Compton scatterings of neutrons and of X-rays are suggested for this proposed experimental test 1. At the present we do not know the velocity distribution of deuterons in metal, which is expected to be different from the Maxwell–Boltzmann distribution for an ideal gas. This experimental demonstration of the BEC of deuterons in a metal based on the velocity distribution may lead to a new discovery. In 1995, this type of experiments for measuring the velocity distribution was used to establish the existence of the BEC of atoms in a magnetic trap at extremely low temperatures, for which the Nobel prize was awarded in 2000.

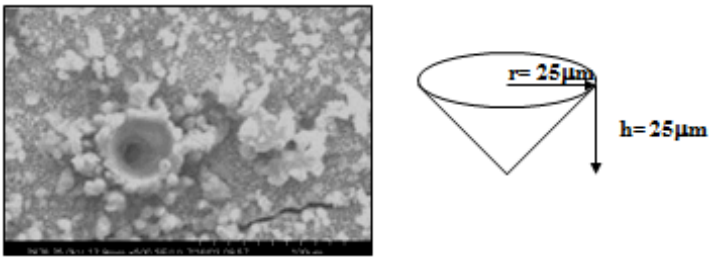

Figure 2. A micro-crator observed in co-deposit electrolysis experiment with applied external electric field [43].

7.2. Proposed Experiment 2

To explore the superfluidity of the BEC of deuterons in metal, experiments are proposed to measure the diffusion rates of both deuterons and protons in a metal as a function of temperature. When the BEC of deuterons in a metal occurs, it is expected that the deuteron diffusion rate will increase substantially more than that of proton. We need to explore a number of other experimental methods for observing the superfluidity, such as the use of torsional oscillators. Experimental demonstration of the superfluidity of deuterons in the BEC state in metal may lead to a new discovery. In 1996, the Nobel prize was awarded for the discovery of superfluidity of ^{3}He.

7.3. Proposed Experiment 3

To explore possibilities of constructing a practical BECNF reactor for energy generation, both experimental and theoretical investigations are proposed to study the possibility of BECNF mini-explosion (or ignition) at extremely low temperatures. At ^{4}He liquid temperature, from estimates of reaction rates using Eq. (12), DD fusions are expected to occur nearly simultaneously from each of micro/nano-scale metal particles contained in a bulk volume. This can cause a mini-explosion (or ignition). An ignition fuel of $\sim$1 cm^3 volume containing $\sim 10^{18}$ of $\sim$10 nm metal particles (each loaded with $\sim 10^{4\sim5}$ deuterons) could be used to ignite $\sim 10^{18}$ DD fusions in a very short time period at ^{4}He liquid temperature or cooling by electromagnetic field gradients, etc. If the proposed experimental test proves this theory to be correct, the ignition fuel can be used in a series of reactor chambers similar to the ignition chamber containing a cryogenic-target at the National Ignition Facility, Livermore National Laboratory [45].

If successful, Proposed Experiment 3 could lead to alternative approach to clean nuclear fusion energy generation technology at commercial and industrial scales.

8. Conclusions

The optical theorem formulation (OTF) of low energy nuclear reactions (LENRs) has been generalized to describe LENRs occurring in deuterium/hydrogen loaded metal systems.

It is pointed out (in Section 3.3) that previous theoretical objections of LENR phenomena made in the past are inappropriate, since they are based on a theoretical description which is not applicable to LENR phenomena.

As a first application of the OTF-LENRs, theory of Bose–Einstein condensation nuclear fusion (BECNF) is developed to explain deuteron-induced nuclear reactions observed in metal. It is based on a single physical observation of deuteron mobility in metals, which may lead to the possibility of Bose–Einstein condensation of deuterons in metals.

It is shown that the BECNF theory is capable of explaining qualitatively or quantitatively all of ten experimental observations (listed in Section 2.2) reported from electrolysis and gas-loading experiments.

It is also shown that observed anomalous tritium and neutron productions can be explained by incorporating a sub-threshold resonance reaction mechanism into the BECNF theory.

The BECNF theory has also predictive powers as expected for a quantitatively predictive physical theory. Experimental tests of theoretical predictions are proposed.

As a potential practical application of BECNF theory, experimental tests of predicted cryogenic ignition are proposed for the purpose of achieving scaling-up of LENRs rates, which may lead to an alternative technology for clean nuclear fusion energy generation at commercial and industrial scales.

Applications of the OTF-LENRs to hydrogen loaded metal systems are in progress.

References

[1] Y.E. Kim, Y.J. Kim, A.L. Zubarev and J.H. Yoon, Optical theorem formulation of low-energy nuclear reactions, *Phys. Rev.* C **55** (1997) 801.

[2] Y.E. Kim and A.L. Zubarev, Nuclear fusion for Bose nuclei confined in ion traps, *Fusion Technol.* **37** (2000) 151.
[3] Y.E. Kim and A.L. Zubarev, Ultra low-energy nuclear fusion of Bose nuclei in nano-scale ion traps, *Italian Physical Soc. Proc.* **70** (2000) 375.
[4] Y.E. Kim and A.L. Zubarev, Equivalent linear two-body method for many-body problems, *Phys. B: At. Mol. Opt. Phys.* **33** (2000) 55–69.
[5] Y.E. Kim and A.L. Zubarev, Ground state of charged bosons confined in a harmonic trap, *Phys. Rev*. A **64** (2001) 013603-1.
[6] Y.E. Kim and A.L. Zubarev, Equivalent linear two-body method for Bose–Einstein condensates in time-dependent harmonic traps, *Phys. Rev*. A **66** (2002) 053602-1.
[7] Y.E. Kim and A.L. Zubarev, *Condensed Matter Nuclear Science*, Proc. 11^{th} *Int. Conf. on Cold Fusion*, Marseilles, France, 31 October–5 November, 2006, World Scientific, New York, pp. 711–717.
[8] Y.E. Kim, Theory of Bose–Einstein Condensation mechanism for deuteron-induced nuclear reactions in micro/nano-scale metal grains and particles, *Naturwissenschaften* **96** (2009) 803and references therein.
[9] Y.E. Kim, Bose–Einstein condensate theory of deuteron fusion in metal, *J. Condensed Matter Nucl. Sci*. **4** (2010) 188, Proceedings of Symposium on New Energy Technologies, the 239th National Meeting of American Chemical Society, San Francisco, March 21–26, 2010.
[10] Y.E. Kim, Theoretical interpretation of anomalous tritium and neutron productions during Pd/D co-deposition experiments, *Eur. Phys. J. Appl. Phys*. **52** (2010) 31101.
[11] Y.E. Kim, Nuclear *reactions in micro/nano-scale metal particles, invited paper presented at the* 5^{th} *asia-pacific conference on few-body problems in physics* (APFB2011), Seoul, Korea, August 22–26, 2011; to be published in the Proceedings of APFB2011.
[12] Y.E. Kim, Cryogenic *ignition of deuteron fusion in micro/nano-scale metal particles, purdue nuclear and many body theory group (PNMBTG) Preprint PNMBTG-11-2011* (November 2011). Invited paper presented at Topical Meeting of the 2012 Nuclear and Emerging Technologies for Space (NETS), the 43rd Lunar and Planetary Science Conference, March 19–23, 2012, the Woodlands, Texas.
[13] W.A. Fowler, G.R. Caughlan and B.A. Zimmermann, Thermonuclear reactions rates, *Annu. Rev. Astron. Astrophys.* **5** (1967) , 525; see also .Thermonuclear reaction rates II, *Annu. Rev. Astron. Astrophys*. **13** (1975) 69.
[14] A. von Engel and C.C. Goodyear, Fusion cross-section measurements with deuterons of low energies, *Proc. R. Soc.* A, **264** (1961) 445.
[15] A.Krauss, H.W. Becker, H.P. Trautvetter and C. Rolfs, Low energy fusion cross-sections of D + D and D + ^{3}He reactions, *Nucl. Phys.* **465** (1987) 150.
[16] M. Fleischman and S. Pons, Electrochemically induced nuclear fusion of deuterium, *J. Electroanal. Chem*. **261** (1989) 301; Errata, *J. Electroanal. Chem.* **263** (1989) 187.
[17] P.L. Hagelstein et al., New physical effects in metal deuterides, *Proc. ICCF-11*, Marseille, France, *Condensed Matter Nuclear Science,* World Scientific, Singapore, 2006, pp. 23–59 and references therein.
[18] Y. Arata and Y.C. Zhang, *J. High Temp. Soc*. **34**(2) (2008) 85.
[19] A. Kitamura et al., *Phys. Lett.* A**373** (2009) 3109, and references therein.
[20] E. Feenberg, *Phys. Rev***. 40** (1932) 40.
[21] A. Coehn, Proof of the existence of protons in metals (with discussion), *Z. Electrochem*. **35** (1929) 676–680.
[22] A. Coehn and W. Specht, Ueber die Beteiligung von Protonen an der Elektrizitaetsleitung in Metallen (Role of protons in electric conductivity of metals), *Z. Phys.* **83** (1930) 1–31.
[23] I. Isenberg, The ionization of hydrogen in metals, *Phys. Rev*. **79** (1950) 736.
[24] P.L. Hagelstein, *Naturwissenschaften* **97** (2010) 345.
[25] E. Storm and C. Talcott, Electrolytic tritium production, *Fusion Technol.* **17** (1990) 680.
[26] K. Cedzynska, S.C. Barrowes, H.E. Bergeson, L.C. Knight and F.W. Will, Tritium analysis in palladium with an open system analytical procedure, *Fusion Technol*. **20** (1991) 108.
[27] F.G. Will, K. Cedzynska and D.C. Linton, Reproducible tritium generation in electrochemical-cells employing palladium cathodes with high deuterium loading, *J. Electroanalytical Chem.* **360** (1993) 161: .Tritium generation in palladium cathodes with high deuterium loading, *Trans. Fusion Technol.* **26** (1994) 209.
[28] J.O'M. Bockris, C.-C. Chien, D. Hodko and Z. Minevski, Tritium and helium production in palladium electrodes and the

fugacity of deuterium therein, *Frontiers Science Series No. 4, Proc. Third Int. Conf. on Cold Fusion.*, October 21–25, Nagoya Japan, Ed. H. Ikegami, Universal Academy Press Tokyo Japan., 1993, pp. 23.

[29] R.Szpak, P.A. Mosier-Boss, R.D. Boss and J.J. Smith, On the behavior of the Pd/D system: evidence for tritium production, *Fusion Technol.* **33** (1998). 38-51.

[30] M. Srinivasan et al., Observation of tritium in gas/plasma loaded titanium samples, *AIP Conf. Proc.* **228** (1990) 514.

[31] A. DeNinno, A. Frattolillo, G. Lollobattista, L. Martinis, M. Martone, L. Mori, S. Podda and F. Scaramuzzi, Emission of neutrons as a consequence of titanium–deuterium interaction, *Il Nuovo Cimento,* **101A** (1989) 841.

[32] T.N. Claytor, D.G. Tuggle, H.O. Menlove, P.A. Seeger, W.R. Doty and R.K. Rohwer, Tritium and neutron measurements from a solid-state cell, LA-UR-89-3946, October 1989, Presented at the NSF-EPRI workshop.

[33] T.N. Claytor, D.G. Tuggle, H.O. Menlove, P.A. Seeger, W.R. Doty and R.K. Rohwer, Tritium and neutron measurements from deuterated Pd–Si, *AIP Conf. Proc.* **228**, Anomalous Nuclear Effects in Deuterium/Solid Systesm, S. Jones, F. Scaramuzzi and D. Worledge (Eds.), Provo Utah, (1990), p. 467.

[34] T.N. Claytor, D.G. Tuggle and S.F. Taylor, Evolution of tritium from deuterided palladium subject to high electrical currents, *Frontiers Science Series No. 4, Proc. Third Int. Conf. on Cold Fusion*., October 21–25 Nagoya Japan, H. Ikegami (Ed), Universal Academy Press, Tokyo, Japan., 1993, p. 217.

[35] T.N. Claytor, D.G. Tuggle and S.F. Taylor, Tritium evolution from various morphologies of deuterided palladium, *Proc. Fourth Int. Conf. on Cold Fusion*, December 6–9, 1993, Maui, Hawaii, T.O. Passel (Ed.), EPRI-TR-104188-V1 Project 3170, Vol 1 7-2 (1994).

[36] T.N. Claytor et al., Tritium production from palladium alloys, *Proc. ICCF-7*, 1998, p. 88.

[37] D.R. Tilley, H.R. Weller and G.M. Hale, Energy level of light nuclei A=4, *Nucl. Phys*. A **541** (1992) 1.

[38] C.E. Rolfs and W.S. Rodney, *Cauldrons in the Cosmos: Nuclear Astrophysics*, University of Chicago Press (1988), chapter 4.

[39] J.M. Blatt and V.F. Weisskopf, *Theoretical Nuclear Physics*, Wiley, 1952,, 8^{th} Printing (1962).

[40] J. R. Oppenheimer and J. S. Schwinger, *Phys. Rev*. **56** (1939) 1066.

[41] G.S. Chulick, Y.E. Kim, R.A. Rice and M. Rabinowitz, Extended parameterization of nuclear-reaction cross sections for few-nucleon nuclei, *Nucl. Phys*. A **551** (1993) 255–268.

[42] P.A. Mosier-Boss, S. Szpak, F.E. Gordon and L.P.G. Forsley, Triple tracks in Cr-39 as the result of Pd–D Co-deposition: evidence of energetic neutrons, *Naturwissenschaften* **96** (2009) 135; .Characterization of Tracks in CR-39 detectors as a result of Pd/D co-deposition, *Eur. Phys. J. Appl. Phys*. **46** (2009) 30901.

[43] S. Szpak, P.A. Mosier-Boss, C.Young and F.E.Gordon, *J. Electroanal. Chem*. **580** (2005) 282.

[44] D.J. Nagel, Characteristics and energetics of craters in LENR experimental materials, to be published; this paper contains many other references on micro-crators.

[45] National Ignition Facility Project: http://www.llnl.gov/nif/nif.html